Analysis of Variability in Additive Manufactured Open Cell Porous Structures

Authors: Sam Evans[1], Eric Jones[1], Pete Fox[1], Chris Sutcliffe[1]

Email: Sam Evans – evanss@liverpool.ac.uk

1 School of Engineering, University of Liverpool, The Quadrangle, Brownlow Hill, United Kingdom L69 3GH

Keywords: Additive Manufacturing, Porous Material, Orthopaedic Materials, Metallic Materials, Photogrammetric Analysis, Porous Inspection, Quality Control

Abstract

In this paper a novel method of analysing build consistency of additively manufactured open cell porous structures is presented. Conventionally methods such as Micro Computed Tomography (µCT) or Scanning Electron Microscopy (SEM) imaging have been applied to the measurement of geometric properties of porous material however high costs and low speeds make them unsuitable for analysing high volumes of components. Recent advances in the image based analysis of open cell structures have opened up the possibility of variation in manufacturing of porous material to be quantified. Here a photogrammetric method of measurement, employing image analysis to extract values for geometric properties, is used to investigate the variation between identically designed porous samples measuring changes in material thickness and pore size, both intra and inter build. Following the measurement of 125 samples intra build material thickness showed a variation of ±12% and pore size, ±4% of the measured mean values across 5 builds. Inter build material thickness and pore size showed mean ranges higher than those of intra build, ±16% and ±6% the mean material thickness and pore size respectively. Acquired measurements created baseline variation values and demonstrated techniques suitable for tracking build deviation and inspecting additively manufactured porous structures to indicate unwanted process fluctuations.

Nomenclature

D_{map}	Distance Map	-
E	Margin of Error	µm
S	Mean Pore Size	µm
T	Mean Material Thickness	µm
$X(\underline{p})$	Centre Point of Circles with Radii Equal to Distance Map Value	Pixels
b	Structuring Element	-
f	Original Image	-
g	Segmented Image	-
k	Threshold Value	-
k^*	Optimum Threshold Value	-
n	Sample Size	-
$\underline{p}$	Point Inside Structure Perimeter	-
$\underline{q}$	Point On Structure Perimeter	-
x, y	Image Kernal Location	Pixels
z	Confidence Level	%
ΔS	Difference in Mean Pore Size	µm
ΔT	Difference in Mean Material Thickness	µm
Ω_R	Distance Ridge Pixels	-
σ	Standard Deviation	µm
$\sigma^2{}_B$	Between-class Variance	-
τ	Mean Thickness	Pixels

Introduction

Increasingly porous materials are finding use in orthopaedic implants as the preferred method for fixing components to host bone, replacing bone screws and cement.[1] The use of open cell porous coatings on implants promotes osseointegration of the bone into the device leading to improved security and longer device lifetime.[2,3] Porous coatings can be produced using various methods including plasma spraying and sintering, however, these current methods do not produce a repeatable structure because of the manufacturing method and this prevents meaningful geometric analysis of the manufactured part, as each is unique.[4]

A method that allows for near identical porous structures to be manufactured is metallic powder based Additive Manufacturing (AM). This method of AM constructs components in a layer-wise fashion by selective melting of successively deposited beds of powder in the required shape with a high power laser until a 3D component is created.[5, 6]

AM allows the manufacturing of complex component geometries, based on 3D Computer Aided Design (CAD) data, without the use of external machining or moulds making it ideal for the fabrication of open cell porous structures such as those used in Orthopaedic implants. Unlike other processes in which porous material is applied to the surface of existing solid components, AM also offers the capability of manufacturing integrated porous and solid material concurrently. Additionally it is possible to create near identical porous structures indefinitely with high repeatability and good control over the structure's properties including porosity, pore size, and homogeneity. However, to make best use of these novel structures it is necessary to determine the reliability of the systems, requiring geometric variation analysis for quality control.

Currently, no standards exist that define methods for non-destructive porous material analysis, with most of the methods used in research slow and difficult to scale for use in high volume production. A low cost rapid measurement system would determine manufacturing fidelity and allow quantified statistical process control to be applied.[7,8]

Currently, three methods are used for porous structure analysis, each capable of non-destructively measuring the required feature size range of these materials. These are: Scanning Electron Microscopy (SEM), Focus Variation (FV), and Micro Computed Tomography (µ-CT). Each system offers advantages and drawbacks depending on the analysis requirements.

SEM analysis uses image data from an electron microscope to determine values for both pore size and strut diameter by measurement of a 1 µm resolution calibrated image, which is carried out manually by drawing lines across struts or pores, selected by the operator, as in Figure 1.[9] This process takes several minutes per image, in addition to the time required for sample preparation and to move parts into and out of the evacuated sample chamber. The higher magnification used (15 to 25X) limits the sampling area, typically to several millimetres squared. With the use of manual measurements and the need to calibrate the microscope magnification the method exhibits significant potential for error. Although the analysis could be automated in a dedicated system, quickly moving specimens in and out of the evacuated chamber sets a significant challenge especially if analysis of more than one type of component is required. Along with manual analysis, measuring a single component can take approximately an hour. The cost of SEM imaging is also significant as they are not readily available in an industrial situation and conversion to a dedicated production line machine would significantly increase the cost further. A typical set of SEM measurements are shown in Figure 1.

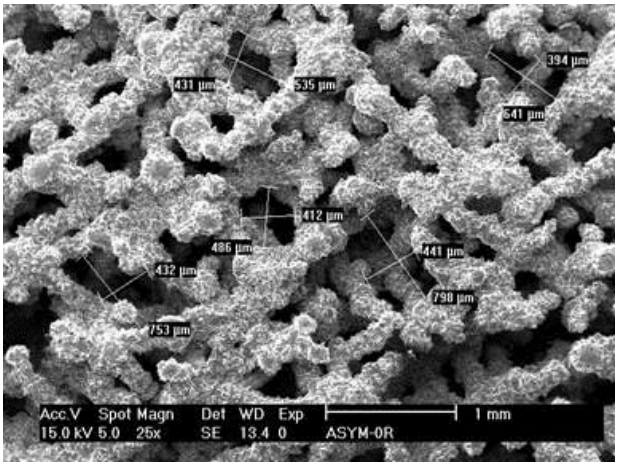

Figure 1: Output from Manual Placement of Measurements on an SEM Image to Measure Pore Size

The Optical Focus Variation method operates by moving the focal plane of a lens, with a very shallow depth of field, through a component, capturing image slices at each position. This gives a series of snapshots where only parts of the rough surface are in focus in any one image. Software is then is then used to construct 3D topographical information from this data, giving a vertical resolution of 10 nm.[10] A typical FV analysis is shown in Figure 2.

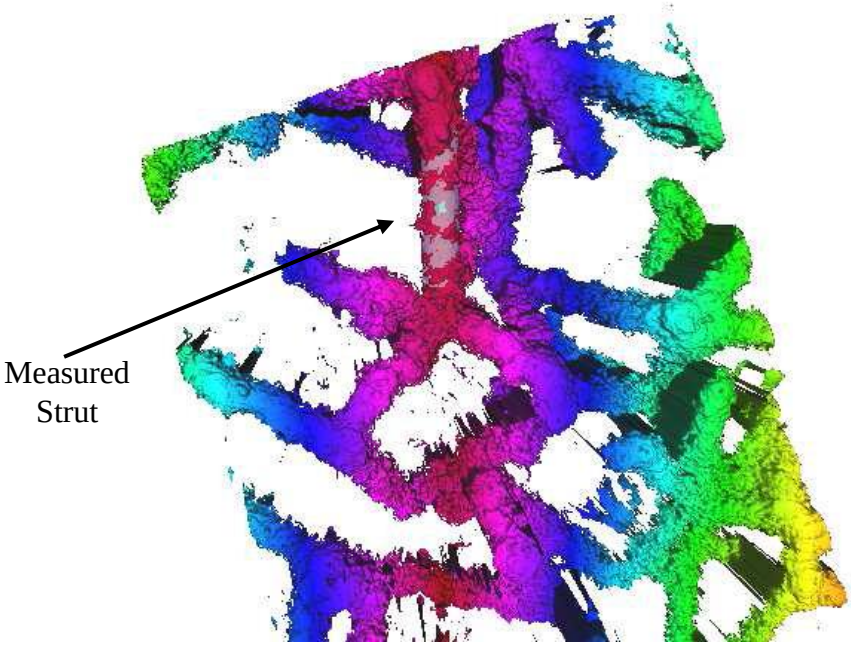

Figure 2: Output from Focus Variation Imaging of a Porous Sample with a Strut Measured for Diameter

The FV system is able to capture data rapidly from the surface of a component and create a 3D model with an overall resolution of 2 µm. However, this method only allows for one strut at a time to be measured due to the need to fit an ideal cylinder to that strut, making the complete analysis of a structure laborious and time consuming, reducing suitability for in-line component inspection.[11] Whilst incredibly rapid in capturing initial images, the cost of the system ranges

in the tens of thousands of pounds alongside the requirement of specific training to capture and process data, taking hours to fully analyse a sample. Both of the techniques are limited to observing the structure near the surface, while µ-CT, explained below, does not suffer from this limitation.

In contrast with other systems, µ-CT is able to internally analyse a 3D porous structure and create a full 3D model of the object. The technique passes X-rays through the part before being detected on the other side. The part is rotated during this process to create the data needed for reconstructing the model. From this pore size, porosity, permeability, build accuracy, and the surface roughness of individual struts can be measured. µ-CT exhibits a high accuracy with a resolution up to 1 µm dependent on the voxel size used to generate the 3D model.[10, 12-15] The process of acquiring and analysing µ-CT data however, can take several hours or even days and cost hundreds of pounds per sample. The method is also computationally demanding requiring large amounts of specialised post processing of the acquired data. The time and cost required for each analysis limits the use of this technology in an industrial environment. A typical set of CT pore size measurements are shown in Figure 3.

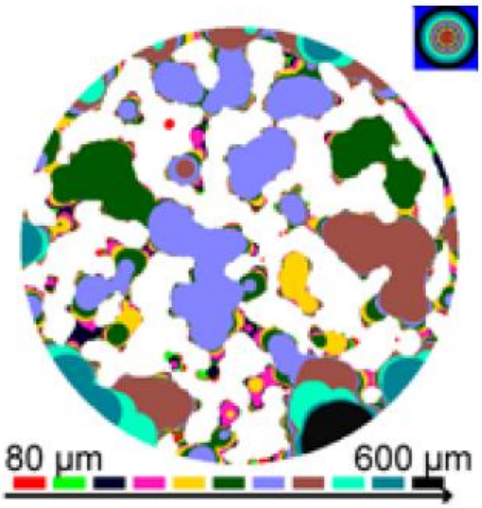

Figure 3: Output of the Pore Size Distribution Analysis of an Open Cell AM Sample [13]

These techniques are useful within a research environment but are less suitable for industry where a low cost, rapid method that opens up such possibilities is required and this method is Photogrammteric Anlaysis.[7,8]

Photogrammetric Analysis is a non-destructive method that captures 2D images of the surface of a porous specimen. It then rapidly analyses the image to determine the material thickness and pore size of the structure. It uses an off-the-shelf DSLR camera or microscope to capture images, while analysis is carried out using open source software and Python code, to extract geometric properties.[7,8] The cost of the high definition camera and macro lens system require a one off investment of several hundred pounds each, while the open source software is free and does not require more than a standard PC to function. This is much less than existing systems. The automated analysis method requires little specific training and ensures the time taken to capture and measure each image takes minutes to produce results.

This paper considers the application of Photogrammetric Analysis to determining variation within structures made using AM and looks to detect differences in what is nominally the same structure, but built at different times and different locations on the build platform. It looks, therefore, to detect relative changes in the structure rather than absolute values of the geometric properties. Although it offers a lower resolution than the existing systems (8 µm compared to less than 2 µm for existing systems) Photogrammetric Analysis has been shown to produce good reproducibility in previous studies, which gives full details of the technique, however, the conclusions of this are also summarised here to demonstrate the reproducibility of the technique this work is dependent on. The method has also been applied to the investigation of less complex periodic Direct Metal Laser Sintered porous components, focusing on accuracy to CAD models with the technique able to demonstrate disparity between vertically and horizontally manufactured struts.[8] Owing to high possible speed, low cost, and rapid post processing, this system is capable of analysing the large numbers of components required for inter and intra build analysis and in-line inspection operations.[7]

This method of quantifying variation finds application in porous, additively manufactured orthopaedic implants, for both human and animal, as well as filtration or electrode production where each part is expected to be identical. It is also likely to be useful in methods such as sintering where the structures are never identical but characterisation of the overall structure is desired. The method could be further applied to any suitably sized and complex structure immeasurable by conventional means in the required large volumes of components.

Materials and Methods

To measure both intra and inter build variability of built structures, 125 porous test specimens were manufactured from Grade 1 Commercially Pure Titanium (CpTi) powder (Sumitomo Corporation, JP) with a mean particle diameter of 45 µm. This consisted of 5 x 5 arrays manufactured across 5 builds to ensure a sufficiently large set of varying samples for statistical analysis. The design of the porous specimens, as shown in Figure 4, consisted of a square porous block, 5 mm thick, surrounded by a 1 mm solid wall with an overlap of 200 µm at solid-porous boundaries to ensure bonding and prevent detachment during handling.

a)

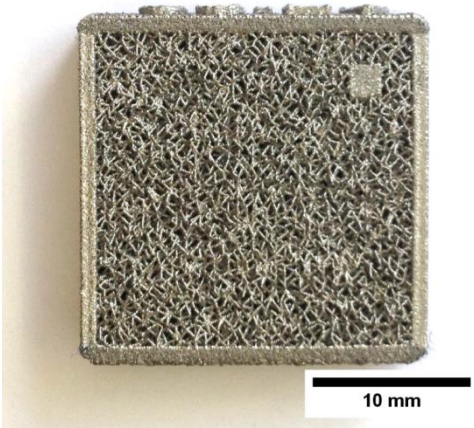

b)

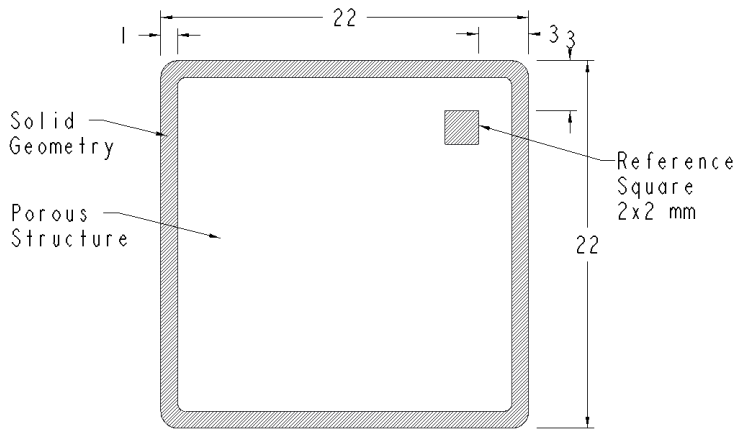

c)

Figure 4: a: Built Porous Specimen, b: Design of the Porous Test Specimen (Dimensions, mm), c: Voxelised Representation of the Porous Structure Design[7]

Samples were manufactured using an MCP Realizer 250 Selective Laser Melting (SLM) system (MCP Tooling Technologies, GB). This method of manufacturing is based upon the melting of 50 µm layers of powder into solid 2D cross section of a component using a high powered laser, of wavelength 1064 nm under an inert atmosphere. Each layer is built upon previously processed material to form a complete 3D component.

The metal lattice samples were generated from data that represented the porous material in the form of a 3D array of point exposures for reduced data size. The structure was designed from the 30% pseudo randomisation of 600 µm cubic unit cells populated with an octahedral shape described by a central node, eight corner nodes and interconnecting struts. This created an

open cell structure designed to mimic human trabecula bone.[6, 9, 16] The generated structure was 'sliced' to the desired layer thickness matching that used for manufacturing (50 μm). The structure was formed by exposing the points to the processing laser so as to create a melt pool, which fused to the underlying material. Struts were formed from six of these pools, with the machine input data controlling angle and spacing. Values for $1/e^2$ (laser spot size defined by intensity), power and exposure time of the laser were optimised to produce near fully dense (at least 99.5%) struts upon solidification of the molten material.[17]

The randomisation of porous structures is controlled by a seeded random number generating algorithm. Computers can either use true random number generators or use algorithms to create data that has the characteristics of random data, known as pseudo random numbers. The randomness of pseudo random data comes from entropy in choosing a start (seed number). If the choice of the seed is random then the data will be the equivalent of random but if the same seed number is used, the data created will always be the same. Thus for a given seed the changes in the structure will always be identical. Applying the same seed to a pseudo random number generator creates an identical list of values controlling the displacement of the nine nodes of the octahedral shape from their original positions. The use of a seeded generator enabled the production of randomised material whilst still allowing the creation of identical structures, if required, by application of the same starting seed. Application of a different random seed would produce a different set of pseudo random values resulting in a similar but not identical porous material.[6, 18] To create multiple parts within a build a single structure file was copied to different locations on the build platform, so the instructions that created each part were identical, and any differences came from the mechanical and optical systems of the AM process.

Samples were identified by both their build and location number. Build numbers ranged from 1-5 and location numbers 1-25. The location of each sample on the build is shown in Figure 5. All samples were built with identical process parameter settings and generated using the same random seed.

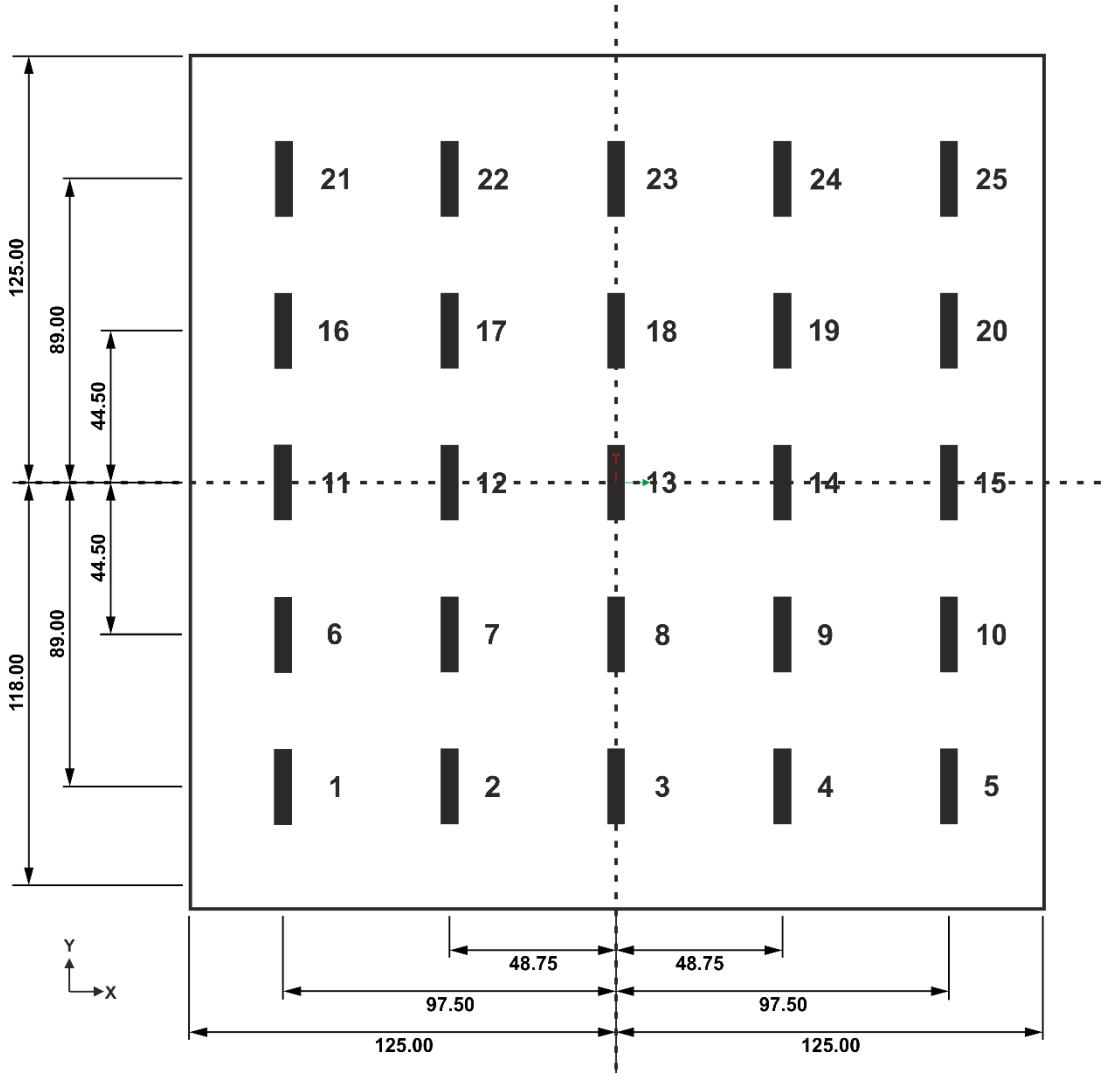

Figure 5: Location of 25 Samples Used in the Variation Study (Dimensions, mm)

Images were captured using a Canon 70D DSLR camera and Canon Macro EF 100 mm lens (Canon Inc., JP). This hardware produced a pixel resolution of 8 µm. The camera was secured in a jig to ensure images of the surface of specimens were captured in a consistent and reproducible manner.[7] Ambient light was used to illuminate the sample and the distance of the lens to the surface of the sample set at 175 mm, the minimum focusing distance, for maximum magnification. Figure 6 shows the jig used in the study. The dimensions selected aligned the central axis of the lens with the centre of the test specimens.

a)

b)

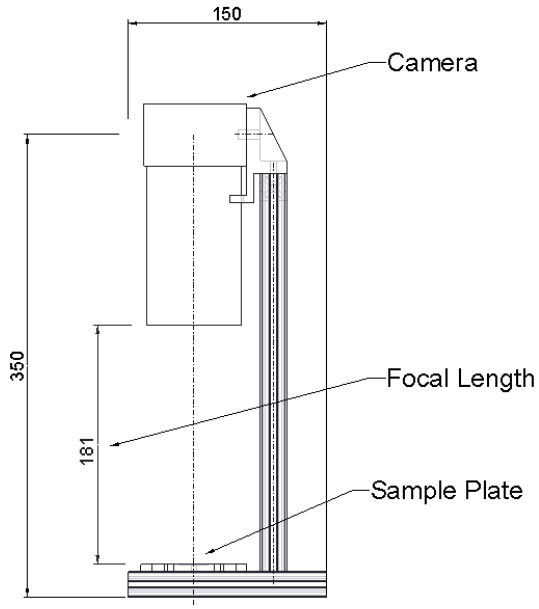

Figure 6: A: Jig Used to Capture Images of Porous Samples, B: Key Dimensions of the Jig Used for Capturing Images (Dimensions, mm)[7]

The camera settings (Table 1) used were selected to ensure that the images were brightly and uniformly lit when photographing at close distances. An exposure value of 6000 ms was used to wash out highlighting of the reflective Titanium and capture the entire surface of the structure.[7]

Table 1: Camera Setting Used to Capture Images of Porous Material[19]

Setting	Value
ISO Speed (-)	1000
Shutter Speed (ms)	6000
Aperture Value (-)	16
Image Format	RAW
Shooting Mode	Timer/Remote

Image Processing Methodology

Following capture images were cropped and converted to 8-bit greyscale, and thresholded using Otsu Binarisation causing struts and nodes of the material to be displayed in white and pores in black in the resulting image.[7, 20, 21]

Thresholding is used to convert an 8-bit greyscale image to black and white by analysing the histogram of the image. During thresholding a value is selected to make areas of the image covered by struts white and those areas covered by pores black by lightening and darkening selected regions. To determine the correct threshold value Otsu Binarisation is used (Equation 1).[20, 21]

$$\sigma^2{}_B(k^*) = \max_{0 \le k \le L-1} \sigma^2{}_B(k) \tag{1}$$

The conditions specified in Equation (1) aim to reduce $\sigma^2{}_B$, the between class variance of an image, to its minimum value by applying different values of k, the threshold value, to achieve the optimum threshold value, k^*. The lowest value indicates the most appropriate value for the threshold, between 0-255 in an 8-bit image histogram, to separates areas of material and pores interpreted as lighter and darker pixels respectively in the image. Areas of material and pores cause two separate peaks to be seen in the histogram, between which the Otsu Binarisation Algorithm locates the optimum threshold value. Otsu Binarisation was carried out on the unique histogram of each image producing individual k^* values. Having selected the k^* value the image is then binarised using Equation (2) and displayed as black and white pixels.[20]

$$g(x,y) = \begin{cases} 1 \text{ if } f(x,y) > k^* \\ 0 \text{ if } f(x,y) \le k^* \end{cases} \tag{2}$$

Equation (2) is used to determine whether a pixel should be assigned the value of 0 (black) or 255 (white) based upon its 8-bit grey value. If the pixel value at location $f(x,y)$ is greater than the optimum threshold value k^* it is made white and given a value of 255. If the pixel is below the threshold value it is instead assigned a value of 0. This divides an image of a porous structure into white areas indicating solid material and black areas indicating pores.[7, 21]

Following thresholding, opening and closing operations were used to remove small noise defects from the image.[7 21] Opening and closing applies dilation (a process in which pixels are

added to the outer perimeter of white areas of a binary image) and erosion (a process in which pixels are removed from the perimeter) to remove small area noise from the image.

Applying an opening filter requires the application of erosion, followed by an equal amount of dilation, denoted by Equation (3).[21]

$$f \circ b = (f \ominus b) \oplus b \tag{3}$$

Equation (3) defines the order of operation for opening of an image, f. $f \ominus b$ indicates the application of erosion to the image, with structuring element, b, controlling where pixels are removed from the edges of white areas, dependent on pixel layout (e.g. wall or corner structures) within a specified area, for the entire image. $\oplus b$ applies an opposing dilation of the image, f, in which pixels are added to edges of white areas, again defined by initial pixel locations and structuring element, b. Similarly a closing filter applies the same procedure but with opposite operations i.e. dilation is performed first, followed by equal erosion as in Equation (4).[21]

$$f \bullet b = (f \oplus b) \ominus b \tag{4}$$

Equation (4), as with Equation (3), indicates the order of the application of erosion and dilation processes. In this case dilation is applied to the edges of white pixels using structuring element, b, followed by a reverse erosion. Erosion and dilation were performed five times for both opening and closing operations, equivalent to five pixels added or subtracted. An image processed as described is shown in Figure 7.

a)

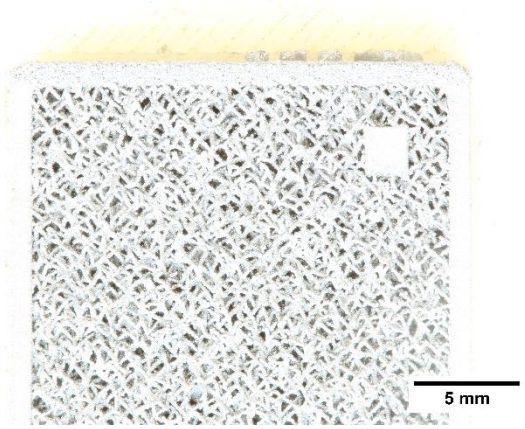

b)

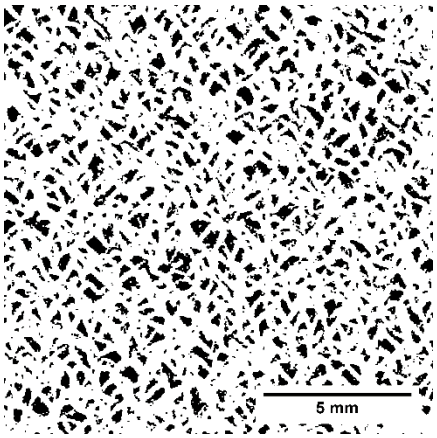

Figure 7: a: DSLR Captured Image of a Porous Sample Prior to Processing, b: Porous Sample Following Cropping, Conversion, Otsu Binarisation, and Filtering

During the noise removal process the geometry of the measured structure is altered. Although this can potentially affect the thickness of the material in the black and white image, the dilation and erosion of five pixels from the starting perimeter is much less than the total width of any structures. For the majority of the image the reverse operation of dilation or erosion accurately returns the structure to its origin following the removal of small areas of noise.

From the processed images two geometric properties were extracted from the porous structures: material thickness and pore size. Material thickness analysis measured the thickness of solid material (white areas) in each image and calculated the distribution and mean diameter. Similarly pore size analysis measured the thickness of the black areas of an image to determine the distribution of pore size and calculate the mean diameter.[7] Both methods of analysis can be used to determine the consistency of manufacturing a porous material during inspection and applied to quantifying the level of variation both intra and inter build.[7]

Material Thickness Analysis Method

Material thickness was calculated using local thickness measurements that analysed the width of solid material, represented as white pixels in images, and calculated a distribution of values. From the processed images a Euclidian distance map was calculated which assigned a value to each pixel, $\underline{p}$, equal to the distance from a black pixel, represented as $\underline{q}$, a point on the perimeter of the structure with a value of 0.[22, 23] From the highest values in the distance map, a distance ridge was calculated to locate the centre of each strut and node formed by white pixels in the image. From each pixel in the distance ridge a circle, equal to the Euclidian distance at that point, was placed. This circle's diameter corresponded to the thickness of the material.[7, 22] Equation (5) represents the algorithm used to calculate local thickness, τ.[23]

$$\tau(\underline{p}) = 2 \cdot \max_{\underline{q} \in X(\underline{p})} (D_{\text{map}}(\underline{q})) \quad (5)$$

Equation (5) calculates the thickness at every location in the set $X(\underline{p})$, a set including all pixels in the calculated distance ridge, using values of the distance map, D_{map}, as the diameter of the circle. Each circle has a centre point in set $X(\underline{p})$, and must exist within the structure i.e. only containing pixels in set, $\underline{p}$, and no pixels

in set, $\underline{q}$. Any pixels in set, $\underline{q}$, indicate the radius of the circle has extended beyond the perimeter of the structure and is therefore invalid.

Equation (6) shows the set $\tilde{X}(\underline{p})$, which represents the points at the centre of all circles with a radius equal to the value of the distance map, contained within the set Ω_R, the pixels in the distance ridge of the structure, and including point $\underline{p}$. Equation (6) is used to specify which pixels in set $\underline{p}$ should be used as points of measuring local thickness by the placement of a circle, primarily to reduce computational time.[23]

$$\tilde{X}(\underline{p}) = \{\underline{x} \in \Omega_R | \underline{p} \in \text{sph}(\underline{x}, D_{\text{map}}(\underline{x}))\} \quad (6)$$

The application of local thickness to a structure is shown in Figure 8 along with key symbols relating Equation (5) and (6) to structure properties.

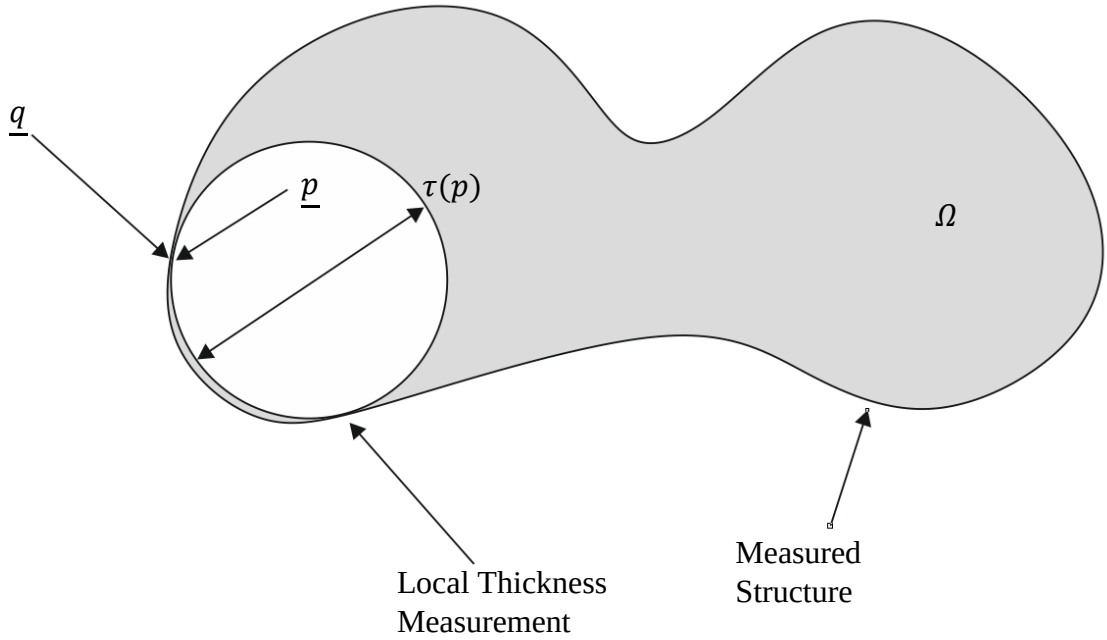

Figure 8: Local Thickness Measurement Process of Structure, Ω adapted from [23]

Following local thickness analysis, a thickness map and distribution of material thickness was created as shown in Figure 9.

a)

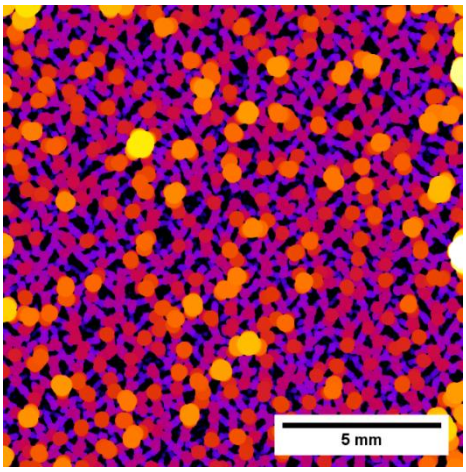

b)

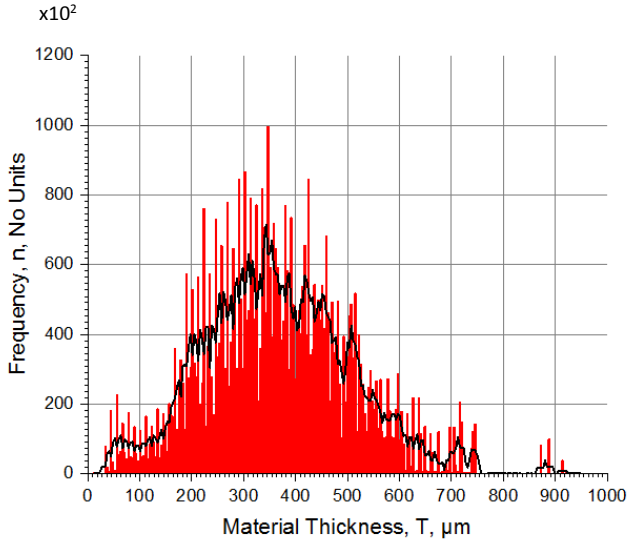

Figure 9: a: Output of Local Thickness Analysis of Material Thickness, b: Accompanying Histogram Showing the Material Thickness Distribution

Pore Size Analysis Methods

Pore size analysis used local thickness algorithms to measure the black areas of each image.[7] Using these measurements a distribution of pore sizes was calculated as shown in Figure 10.

a)

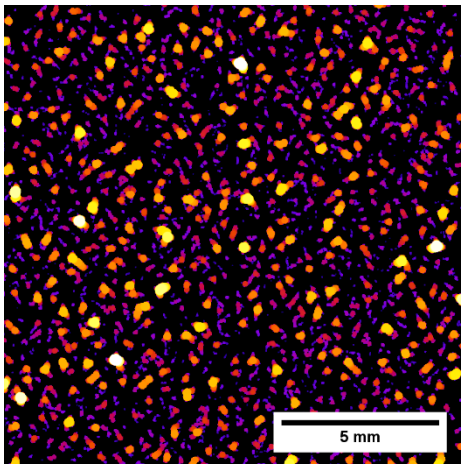

b)

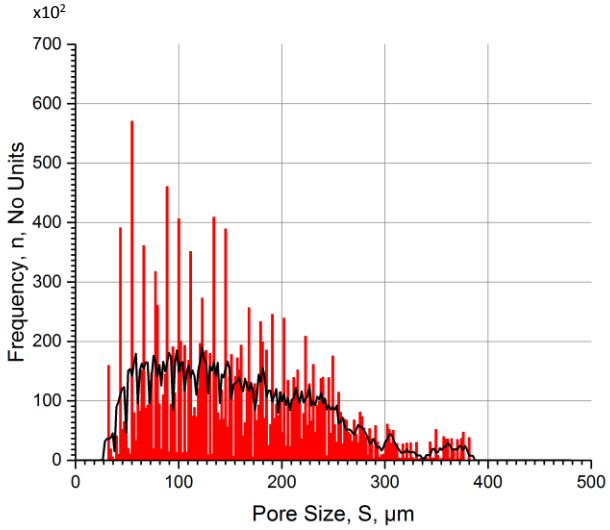

Figure 10: a: Output of Local Thickness Analysis of Pores, b: Accompanying Histogram Showing the Pore Size Distribution

The technique described was validated by comparing the results from Photogrammetric Analysis against the standard technique of SEM image analysis. Both the absolute measured size (material thickness, pore size) and the variability (standard deviation) in these measurements were determined. Validation was in two forms, one to compare the values measured between the two techniques, and the second to determine reproducibility when re-measuring the same sample, determining the sensitivity of the technique to the loading and unloading of specimens. This second validation was achieved by loading measuring and unloading the same specimen twelve times, for four different samples. In the comparison with SEM it was found that the measured material thickness was significantly different, approximately double. This occurred because of the presence of sintered on powder on the surface of the strut, and thicker nodes, as in Figure 1. The Photogrammetric Analysis technique includes the sintered on powder and node thickness in the calculation of material thickness, while the SEM technique did not. However, it was observed that the values obtained by Photogrammetric Analysis were consistent and there was little variability between tests.

Sample data is included in Table 2 for the material thickness for four different samples, the Photogrammetric Analysis being carried out twelve times and the SEM measurements being made on twenty struts and twenty pores. Table 3 shows the data for pore size which again shows a high degree of repeatability.[7]

Table 2: Material Thickness Measurements Obtained from Imaging and SEM Analysis of Four Porous Samples [7]

Measurement Method	Sample No.	Mean Material Thickness, T, μm	Standard Deviation, σ, μm
Photogrammetric Technique	1	417	9
	2	412	7
	3	428	5
	4	431	6
SEM	1	206	12
	2	178	15
	3	220	25
	4	219	21

Table 3: Pore Size Measurements Obtained from Imaging Analysis of Four Porous Samples and SEM Analysis [7]

Measurement Method	Mean Pore Size, S, μm	Standard Deviation, σ, μm
Photogrammetric Technique	158	2
SEM	450	110

The high variation seen in SEM images was a result of the lack of automation or repeatability in the manual selection of measurement locations. This, coupled with the randomised nature of the structure, causes a wide range of values to be measured. For pore size in particular the inconsistent and unsymmetrical geometry and shape of the material make it difficult to select measurement locations that produce low deviation in results.

The accuracy of the technique was also demonstrated using a standard resolution test reticle (graticule) of known dimension, with measurements between 208 and 63 μm showing a mean error of 2.7 μm. The minimum resolvable feature size of 18 μm due to pixel size of the camera and lens set. Between 63 μm and 18 μm the system sometimes failed to differentiate lines of similar thickness (within 8μm of each other). Although unable to differentiate similarly sized features in the lower range, the system was still capable of measuring across, or even higher than, the range of 18–208 μm, in which the majority of feature sizes for porous material are contained. [7]

Both the low deviation and high accuracy of the system make it ideal for variation analysis, and in particular for quantifying the range of material thickness and pore size for each build produced, where precise measurements of a maximum and minimum values of component geometries are required for meaningful comparison.

All samples manufactured in the study described here were imaged four times to achieve statistically significant measurements calculated from Equation (7) using a margin of error of 5 μm and a confidence interval of 90 %.[24]

$$n = \frac{z^2\sigma^2}{E^2} \tag{7}$$

Here, n, represents the minimum number of samples required to achieve a specific statistical significance, z, with a selected maximum margin of error, E. The value calculated is dependent on the standard deviation, σ, of the imaged based measurement system.[24]

The mean values and standard deviation of material thickness and pore size were calculated for each sample. Analysis of variance (ANOVA) statistical testing was performed for both intra and inter build analysis to determine any statistical significance between the measured means of the components for both material properties. ANOVA testing used a 95% confidence level as a measure of significance.[24] Post-hoc analysis using Turkey's HSD (Honest Significant Difference) test was also applied to the data to determine which mean value pairs were significantly different from one another.[25]

Results

Intra build analysis was investigated to quantify variation between the 25 components manufactured for each of the five builds. Variation for material thickness and pore size was assessed for each build and ANOVA performed to indicate any statistically significant differences between components. All 25 components were compared to one another and the range of variation measured. Following this, each of the 25 part locations were analysed inter build to measure the variation at each point on the build plate.

Intra Build Variation

Intra build variation compared all 25 samples across a bed to analyse the variation of the measured means for material thickness and pore size, to show the presence of similarities or differences between samples within a build and produce a baseline for comparing samples manufactured simultaneously. Results for mean measured values, the standard deviation, and the range of measured values were calculated for each analysed property.

Material Thickness Intra Build Variation

Analysis of material thickness compared 25 samples across each build to determine the variation in the measured mean. Results for intra build material thickness are shown in Table 4.

Table 4: Variation of Intra Build Material Thickness Across Five Builds

Build	Mean Material Thickness, T, µm	Standard Deviation, σ, µm	Material Thickness Range, ΔT, µm
1	383	31	119
2	356	19	75
3	414	30	137
4	344	8	31
5	301	21	66

From Table 4 the amount of variation within each build is observed. The mean diameter of all five builds was calculated as 360 µm with a deviation of 38 µm. The maximum measured range for material thickness seen within a build was 137 µm for build 3. The mean range across all builds was 85 µm with a deviation of 38 µm. ANOVA testing of the mean material thickness values for each location on the build determined no significant differences intra build.

Pore Size Intra Build Variation

Results for pore size compared 25 samples across each build to determine the variation in mean size. Results for intra build pore size are shown in Table 5.

Table 5: Variation of Intra Build Pore Size Across Five Builds

Build	Mean Pore Size, S, µm	Standard Deviation, σ, µm	Pore Size Range, ΔS, µm
1	147	6	24
2	155	5	18
3	147	2	9
4	160	3	10
5	165	3	8

From Table 5 the amount of variation within each build is observed. The mean pore size for all five builds was calculated as 155 µm with a deviation of 7 µm. The maximum measured range for pore size seen within a build was 24 µm for build 1. The mean range across the builds was 13 µm with a deviation of 6 µm. ANOVA testing of the mean pore size values for each location on the build determined no significant differences intra build.

Inter Build Variation

Inter build variation analysis compared 25 locations between five builds to measure the difference in the material thickness and pore size. The maximum difference in measurements and the locations of maximum and minimum variations were calculated for both properties of the porous.

Analysis of material thickness compared 25 samples locations through five builds to observe variation in the measured mean material thickness. Results for inter build material thickness and pore size are shown in Figure 11a and 11b respectively.

a)

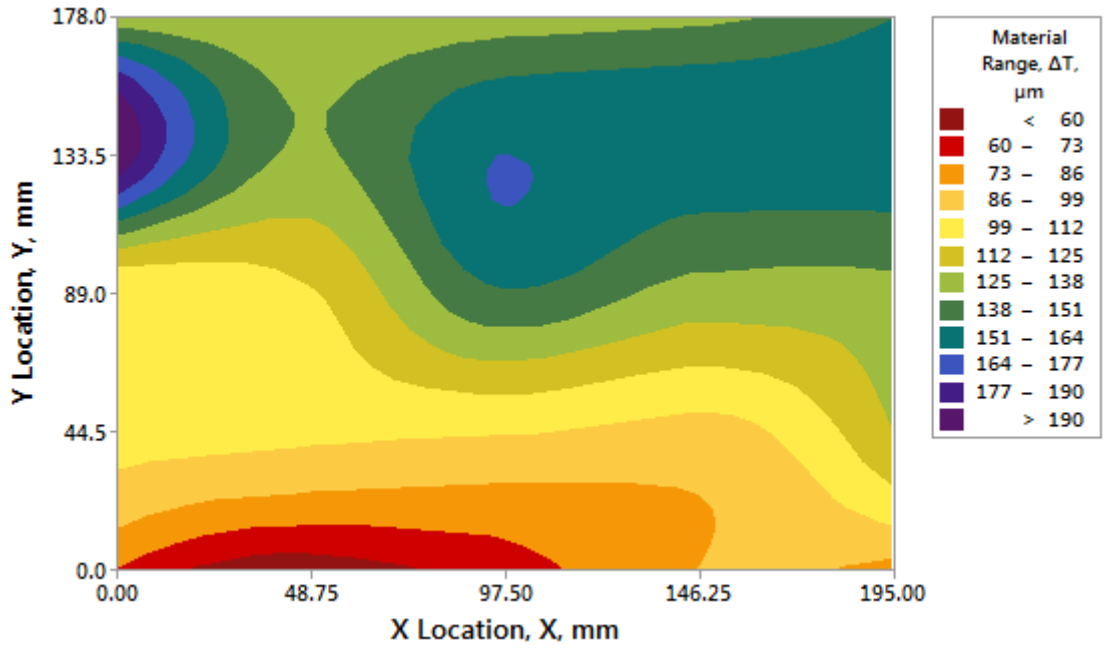

b)

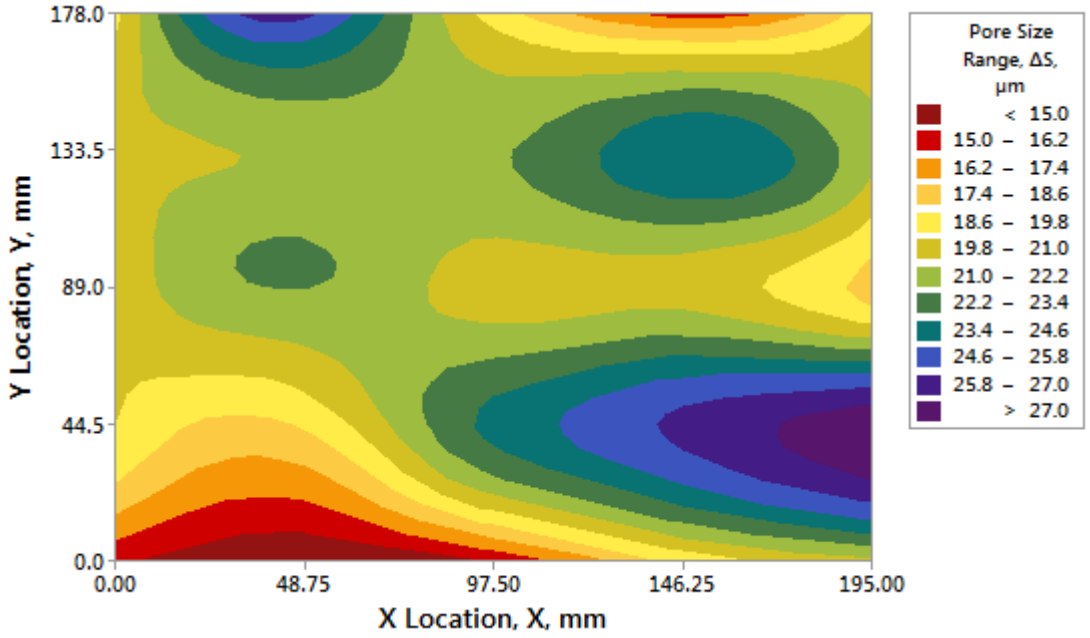

Figure 11: a: Mean Material Thickness Measured at 25 Locations Between Five Builds, b: Mean Pore Size Measured at 25 Locations Between Five Builds

Figure 11a shows the maximum measured difference in material thickness, 200 µm, was located at position 16 with the minimum value of 52 µm located in position 2. The mean measured difference between builds was calculated as 20 µm with a deviation of 34 µm. ANOVA testing of the mean material thickness values for each location on the build determined the existence of significant differences inter build. A Post-hoc Turkey HSD test showed all measured means for each build to be significantly different from all other builds except for build 2 and 4.

Figure 11b shows the maximum measured range in pore size, 28 µm, was located at position 10 with the minimum value of 14 µm located in position 2. The mean measured difference between builds was calculated as 21 µm with a deviation of 3 µm. ANOVA testing of the mean pore size values for each location on the build determined the existence of significant differences inter build. A Post-hoc Turkey HSD test showed all measured means for each build to be significantly different from all other builds except for build 1 and 3.

Discussion

The results presented quantify the baseline variation in the additive manufacturing of open cell porous material, from which variation tracking and go/no go inspection can be carried out, and the capabilities of the fabrication equipment to consistently reproduce parts.

Intra build analysis showed some variation for both material thickness and pore size. For material thickness a mean value of 360 µm was calculated for all 125 samples manufactured. The mean range in which the measured values lay was calculated as 85 µm, equivalent to 12% above or below the mean diameter. The variation between the measured material thickness showed no location within the build plate produced components of a significantly different mean value following ANOVA.

Pore Size analysis showed a mean value of 155 µm. The mean range of measured values was 13 µm, 4% above or below mean pore size. Pore size showed no significant difference in mean values between locations for any build.

Inter build analysis, showed significant differences between a number of builds for both material thickness and pore size. The maximum measured range in material thickness for inter build analysis was 120 µm, indicating up to a 16% variation above or below the mean material thickness. Similarly, pore size analysis showed a higher mean range for inter build analysis with a value of 21 µm, 6% variation above or below the mean, indicating a larger variation in the measured size of the structure.

This outcome follows expectation as all components within a build are subjected to the same or similar conditions whilst being manufactured simultaneously. Inter build components however, are much less likely to be built under identical conditions having been manufactured at different times, accounting for the higher variation in both material thickness and pore size.

Contour plots generated from inter build data also show areas of peak similarity or dissimilarity between components. In particular the lower left area of the build shows the least difference between measured means whereas the upper left, upper right, and lower right all show a higher range where analysed structures vary the most. This localisation of variation may be caused by fluctuations in conditions that differ more between builds in particular areas of the platform such as inert gas flow.

The methods demonstrated in this paper can be applied to both the tracking of variation over time for additively manufactured open cell porous structures and go/no go inspection where more expensive or time consuming methods would be impractical. By frequently building identical components the measured values for material thickness and pore size can be used to determine if any unwanted changes have occurred in build parameters or environment that would adversely affect the manufacture of the porous structure. The measurements taken can be compared to a baseline determined previously, such as the one presented in this paper, which provides a value of expected variation for a machine or even specific build layout. A

measured test specimen falling outside this level of variation would indicate the requirement for service or adjustment to the manufacturing process.

Likewise when applied to go/no go inspection of individual components, measurements taken can again be compared to a known baseline of variation or a predetermined minimum or maximum value for material thickness or pore size. Any components outside of the required values would fail inspection and potentially indicate issues with the AM build. This baseline can also be used to measure if any changes made to the build process cause an increase or decrease in variation and therefore the performance capabilities of the machine. Only with the use of a high speed, low cost measuring technique, such as the one used in this study, can a suitable number of components be measured to statistically analyse variation both intra and inter build. Further operator subjectivity can be removed by using a CAD generated template to overlay with measured data to quantify the relative similarity/dissimilarity of the local are under investigation.

Statistically significant differences seen when analysing inter build variation of additively manufactured porous material demonstrate the requirement for high volume inspection of components with the aim of indicating unwanted fluctuations in the quality of the fabrication process and resulting parts. With the data collected used as a comparable set, components not suitable for application may be identified, indicating issues with the manufacturing process such as: incorrect parameters used in structure generation, broken or damaged struts, change in laser power, or unfavourable chamber conditions.

Conclusions

A method of analysing inter and intra build variation with respect to material thickness and pore size using a recently developed technique for rapid analysis of porous material has been demonstrated. This method is capable of tracking changes in porous structures caused by fluctuations in build conditions both intra and inter build for large volumes of components. Analysis of 125 specimens showed the mean variation across a build and the mean variation between builds for both measured properties. For intra build material thickness a mean range of 85 µm was measured equating to limits 12% higher or lower than mean measured value. The mean inter build range for material thickness was calculated as 120 µm, 16% higher or lower than the mean range for intra build. A higher variation was seen between builds than within builds and following ANOVA testing inter build variation was shown to be significantly different whereas intra build mean values were not.

Intra build analysis of pore size showed a mean range of 13 µm across the five builds, 4% above or below the measured mean pore size. For inter build analysis pore size ranges had a mean value of 21 µm, 6% above or below the mean. As with material thickness, pore size measurements showed intra build mean values to not be significantly different following ANOVA testing, contrary to inter build mean values.

Using this technique, a component containing porous material may be inspected and determined to be in or out of a specified tolerance for each property of the material (material thickness and pore size) and in the event of failure, build parameters adjusted to ensure parts meet the required manufacturing specification. Due to the rapid and low cost nature of the photogrammetric technique used, this method of analysis is suitable for high volumes of components allowing a large amount of data to be gathered and changes in the measured properties of the material tracked over a prolonged period of time. The method of analysis can be incorporated into existing inspection protocols enabling porous material to undergo measurement alongside the solid structures in an orthopaedic component, and other

applications, contrary to the current methods of measuring only a small number sample to determine properties due to high cost and time requirements. Using an automated image based method, measurements are performed consistently and reproducibly, and the method can therefore be considered for use as a tracking tool for process variability and go/no go inspection for a modest capital outlay (<£1K) and at a rapid turn-around (few minutes per sample at most).

Funding

This research received no specific grant from any funding agency in the public, commercial, or not-for-profit sectors.

Declaration of Conflicting Interests

The Authour(s) declare(s) that there is no conflict of interest.

References

1. Friedman RJ, Black J, Galante JO, Jacobs JJ, Skinner HB. Current Concepts in Orthopaedic Biomaterials and Implant Fixation. Journal of Bone and Joint Surgery-American Volume. 1993;75A(7):1086-109.
2. Bobyn JD, Toh K, Hacking SA, Tanzer M, Krygier JJ. Tissue Response to Porous Tantalum Acetabular Cups: A Canine Model. The Journal of Arthroplasty. 1999;14(3):347-54.
3. Jeyapalina S, Beck JP, Bloebaum RD, Bachus KN. Progression of Bone Ingrowth and Attachment Strength for Stability of Percutaneous Osseointegrated Prostheses. Clinical Orthopaedics Related Research. 2014;472(10):2957-65.
4. Ryan G, Pandit A, Apatsidis DP. Fabrication Methods of Porous Metals for Use in Orthopaedic Applications. Biomaterials. 2006;27(13):2651-70.
5. Gebhardt A. Rapid Prototyping. Hanser Publishers. 2003.
6. Robinson J. Optimisation of the Selective Laser Melting Process for the Production of Hybrid Orthopaedic Devices. PhD Thesis, The University of Liverpool. 2014. [Unpublished].
7. Evans S, Jones E, Fox P, Sutcliffe C. Quality Control of Metallic Open Cell Porous Structures Fabricated via Additive Manufacturing. 2017. [Unpublished].
8. Vanderesse N, Ky I, Quevedo González F, Nuño N, Bocher P. Image Analysis Characterization of Periodic Porous Materials Produced by Additive Manufacturing. Material & Design. 2016;92:767-78.
9. 15. Mullen L, Stamp RC, Fox P, Jones E, Ngo C, Sutcliffe CJ. Selective Laser Melting: A Unit Cell Approach for the Manufacture of Porous, Titanium, Bone In-Growth Constructs, Suitable for Orthopedic Applications. II. Randomized Structures. Journal of Biomedical Materials Research Part B-Applied Biomaterials. 2010;92B(1):178-88.

10. Leach R. Optical Measurement of Surface Topography. Springer Berlin Heidelberg. 2011.

11. Danzl R, Helmli F, Scherer S. Focus Variation—A Robust Technology for High Resolution Optical 3D Surface Metrology. Strojniski Vestnik 2011;57(03):245-56.

12. Yan C, Hao L, Hussein A, Raymont D. Evaluation of Cellular Lattice Structures Manufactured using Selective Laser Melting. International Journal of Machine Tools and Manufacture. 2012;62:32-8.

13. Jones JR, Atwood RC, Poologasundarampillai G, Yue S, Lee PD. Quanitfying the 3D Macrostructure of Tissue Scaffolds. Journal of Material Sciience: Materials in Medicine. 2009;20(2):463-71.
14. Kim TB, Yue S, Zhang Z, Jones E, Jones JR, Lee PD. Additive Manufactured Porous Titanium Structures: Through-process Quantification of Pore and Strut Networks. Journal of Materials Processing Technology. 2014;214(11):2706-15.

15. Yue S. Non-Destructive Quantification of Tissue Scaffolds and Augmentation Implants Using X-Ray Microtomography. PhD Thesis, Imperial College London. 2011.

16. Mullen L, Stamp RC, Brooks WK, Sutcliffe CJ, Jones E. Selective Laser Melting: A Regular Unit Cell Approach for the Manufacture of Porous, Titanium, Bone In-Growth Constructs, Suitable for Orthopedic Applications. Journal of Biomedical Materials Research - Part B Applied Biomaterials. 2009;89(2):325-34.
17. Steen W, Watkins KG, Mazumder J. Laser Material Processing. Springer London. 2010.
18. Brooks W. The Creation of Lattice Structures Using Selective Laser Melting. University of Liverpool. 2011. [Unpublished Thesis].
19. Canon Inc. Canon EOS 70D Instruction Manual. 2015. Available from: http://www.canon.co.uk/ [Accessed 08 June 2016].
20. Rasband, W.S., ImageJ, U. S. National Institutes of Health, Bethesda, Maryland, USA, http://imagej.nih.gov/ij/, 1997-2016.

21. Gonzalez RC, Woods RE. Digital Image Processing. Pearson/Prentice Hall. 2008.

22. Dougherty R, Kunzelmann KH. Computing Local Thickness of 3D Structures with ImageJ. Microscopy and Microanalysis. 2007;13(SupplementS02):1678-9.
23. Hildebrand T, Rüegsegger P. A New Method for the Model-Independent Assessment of Thickness in Three-Dimensional Images. Journal of Microscopy. 1997;185(1):67-75.
24. Mann PS. Introductory Statistics. John Wiley & Sons. 2010.

25. Turkey J. Comparing Individual Means in the Analysis of Variance. Biometrics. 1949;5(2):99-114.